Fuel 346 (2023) 128404

Contents lists available at ScienceDirect

Fuel

journal homepage: www.elsevier.com/locate/fuel

Full Length Article

Optimization of biodiesel production from rice bran oil by ultrasound and infrared radiation using ANN-GWO

A.H. Sebayang [a], Fitranto Kusumo [b], Jassinnee Milano [c,*], A.H. Shamsuddin [c], A.S. Silitonga [b,d,*], F. Ideris [c], Joko Siswantoro [e], Ibham Veza [f], M. Mofijur [b,g], Shir Reen Chia [c]

[a] Department of Mechanical Engineering, Politeknik Negeri Medan, 20155 Medan, Indonesia
[b] Centre for Technology in Water and Wastewater, School of Civil and Environmental Engineering, University of Technology Sydney, Ultimo, NSW 2007, Australia
[c] Institute of Sustainable Energy, Universiti Tenaga Nasional, 43000 Kajang, Selangor, Malaysia
[d] Center of Renewable Energy, Department of Mechanical Engineering, Politeknik Negeri Medan, 20155 Medan, Indonesia
[e] Department of Informatics Engineering, Faculty of Engineering, Universitas Surabaya, Jl. Kali Rungkut, Surabaya 60293, Indonesia
[f] Department of Mechanical Engineering, Universiti Teknologi PETRONAS, 32610 Bandar Seri Iskandar, Perak Darul Ridzuan, Malaysia
[g] Mechanical Engineering Department, Prince Mohammad Bin Fahd University, Al Khobar, Saudi Arabia

ARTICLE INFO

Keywords:
Non-edible oil
Statistical study
Hybrid methods
Parameters study
High conversion rate

ABSTRACT

A system combining ultrasound and infrared radiation was used to increase the chemical reactions between incompressible reactants by enhancing their mass transfers with the aim to reduce the energy usage and reaction time. In this study, biodiesel from RBO was produced via transesterification, and the process variables were optimized using the combination of ANN and GWO algorithm. Process parameters considered in this study are ratio of methanol to oil, catalyst concentration, and reaction time. Based on the ANN-GWO algoritm used, the optimum conditions for the process parameters were (1) methanol to oil ratio: 60%, (2) concentration of catalyst: 1 wt%, (3) time: 7.76 min, leading to the metyl ester yield of 98.16 wt%. The algoritm was verified by conducting a triplicate independent experiments using the suggested optimum values, resulting in an average methyl ester yield of 97.74 wt%. Subsequently, properties of rice bran biodiesel were compared to ASTM D6751 and EN 14214 standards, and the obtained values met both the standards.

1. Introduction

In the last decades, renewable energy has obtained considerable global attention as an alternative to fossil fuels due to the increasing energy demands and awareness of environmental damages resulting from prolonged usage of fossil fuel. As a result, renewable energy in form of sea wave, wind, solar, hydro, and geothermal are being implemented worldwide [1–3]. In addition, biofuels such as biodiesel and bioethanol, which are easily stored and transported are considered as alternatives to be utilized in transportation sector. Biodiesels are long-chain fatty acids of mono-alkyl esters typically produced from animal fats or vegetable oils that posseses beneficial fuel properties similar to petroleum diesel [4–8]. Several methods, such as pyrolysis, dilution, and microemulsion, can be used to convert triglycerides in vegetable oils to methyl esters [9–12]. However, commercialized biodiesel production field typically uses esterification and transesterification, as compared to other methods [13–15].

The main challenge in producing biodiesel is the insolubility between oil and alcohol, which can inhibit the process of mass transfer and reduce the rate of reaction. Hence, it is imperative to enhance the reaction by using improved technology. Microwave, ultrasound, infrared radiation techniques and non-catalytic supercritical are among the popular methods [14,15]. Many successful studies apply ultrasonic methods for biodiesel production [16,17]. Via ultrasound-assisted process, tiny bubbles are created by continous expansion and compression in the solvent. These bubbles keep expanding, leading to the buildup of energy in the bubbles until their subsequent collapse. This is commonly referred to as an acoustic cavitation (Fig. 1) [18]. Via this, liquid solvent is affected both physically and chemically [19,20]. As a result, methyl ester yields will be higher, reaction times will be shorter, the amount of

* Corresponding authors at: Centre of Green Technology, Faculty of Engineering and Information Technology, University of Technology Sydney, NSW 2007, Australia (A.S. Silitonga).
E-mail addresses: jassinneemilano@hotmail.com, jassinneemilano.jm@gmail.com, jassinnee.milano@uniten.edu.my (J. Milano), ardinsu@yahoo.co.id (A.S. Silitonga).

https://doi.org/10.1016/j.fuel.2023.128404
Received 5 December 2022; Received in revised form 4 April 2023; Accepted 10 April 2023
Available online 19 April 2023

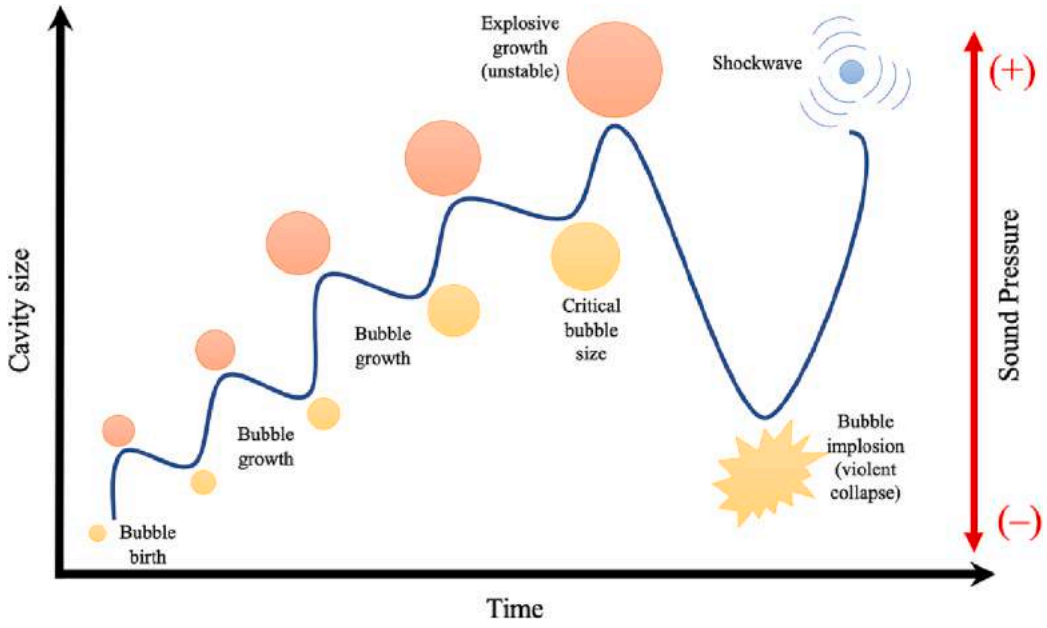

Fig. 1. Acoustic cavitation of ultrasonic waves.

catalyst used will be lowered, and less energy will be used. The usage of ultrasound as an intensification technique in transesterification reaction contributes to only a small increase in biodiesel production cost (0.08–0.5%), when compared to conventional heating [21]. The infrared radiation-assisted reactor is in the same boat. With the range of energy between 0.001 and 1.7 eV, infrared radiation can penetrate deeper into reactant and intensively absorbed [22]. Therefore, this energy could lower reaction temperatures and minimize the amount of energy consumed by reactant molecules, which is the most essential component in enhancing biodiesel quality [20,23]. This process has been utilized to convert waste goat tallow into biodiesel, producing sufficient yields in a shorter time than the traditional method [24]. Furthermore, the energy usage for a transesterification reaction using infrared radiation was reported to be only 25% as compared to conventional heating [25]. Hence, a combination of both ultrasound and infrared radiation is expected to provide significant time and energy saving in producing biodiesel.

To date, various waste and non-edible oil feedstocks such as Jatropha [26,27], Calophyllum inophyllum [18], waste cooking oil [28], rubber seed [29], waste coffee ground [30] and rice bran oil [31] have been researched. Rice bran oil (RBO) is a by-product from the milling process of paddy rice, obtained from the grain's hard outer layers [32]. This non-edible oil is often discarded as agricultural waste. China and India produce the most RBO, and a global production of RBO is conservatively estimated to be not less than 7.5 million metric tons annually [33]. In a study, it was found that a volumetric blend of 20 % RBO and 80 % petrodiesel is the most economically effective to be used in the existing diesel engines [34]. Hence, RBO is a suitable candidate for sustainable biodiesel feedstock, since it is abundantly available and unsuitable to be consumed by human [35].

In order to obtain maximum biodiesel yield with minimal usage of resources, experiments and methods need to be properly planned. Optimization techniques utilizing both linear and nonlinear equations are ideal for this purpose since they are simple to examine and able to solve huge complicated conditions. For the past few years, artificial neural networks (ANN) has gained widespread recognition as a modeling technique for simulating complicated situations [17,36]. Using artificial intelligence, ANN offers series of advantages as compared to the traditional modeling tools. It is easier to understand both phenomenological and mathematical context of the conditions that have to be dealt with by using ANN, without making unnecessary assumptions. Linear and nonlinear correlations of the process parameters can be simultaneously studied directly from a collection of conditions. ANN can comprehend a large number of factors in a relatively quick manner, resulting in precise predictions utilizing inputs from the user. In addition, ANN can also understand nonlinear correlations between the various diverse inputs related to a biological system. One of the primary benefits of utilising ANN for modelling complex systems is the capability to operate without complicated physical equations, initial boundary conditions, or starting assumptions about the make-up of the function or data distribution [6].

Furthermore, ANN may be simulated using a set of available experimental data, without the need to thoroughly understand the chemical/biological process being mimicked [37]. Hence, experimental conditions obtained from tools such as Box-Behnken design can be used in ANN. Compared to other mathematical models, ANN has a better tolerance for errors due to its capacity to build on partial knowledge. In addition, ANN has also been utilized in optimizing process parameters for biodiesel production [38,39]. Therefore, ANN is a helpful modeling tool in forecasting and optimizing complex process parameters. In a study, heterogeneous catalysts was employed to produce biodiesel from low-grade oil using ANN and response surface methodology (RSM) [40]. The results demonstrated that ANN's prediction performance was superior to RSM's. Furthermore, an investigation was conducted by Onukwuli et al. (2021) by utilizing both RSM and ANN-GA in forecasting optimum conditions for producing biodiesel using oil obtained from *Chrysophyllum albidum* seed [41]. From the study, it was concluded that ANN had higher correlation coefficients, resulting in faster reaction time, less energy, less catalyst, with higher yield compared to RSM in optimal condition.

A metaheuristic is an algorithmic framework inspired by nature to find a near-optimal solution to an optimization issue. By such, grey wolf optimizer (GWO) is based on population metaheuristic which imitates how a pack of grey wolves behave when hunting a prey [40,41]. Comparatively, it is found that GWO requires less modified parameters, while outperforms other evolutionary computation-based methodologies, including particle swarm optimization (PSO), fast evolutionary programming (FEP), and gravitational search algorithm (GSA) [42].

The aim of this study is to evaluate the effectiveness of combining ultrasound and infrared radiations for biodiesel production from rice

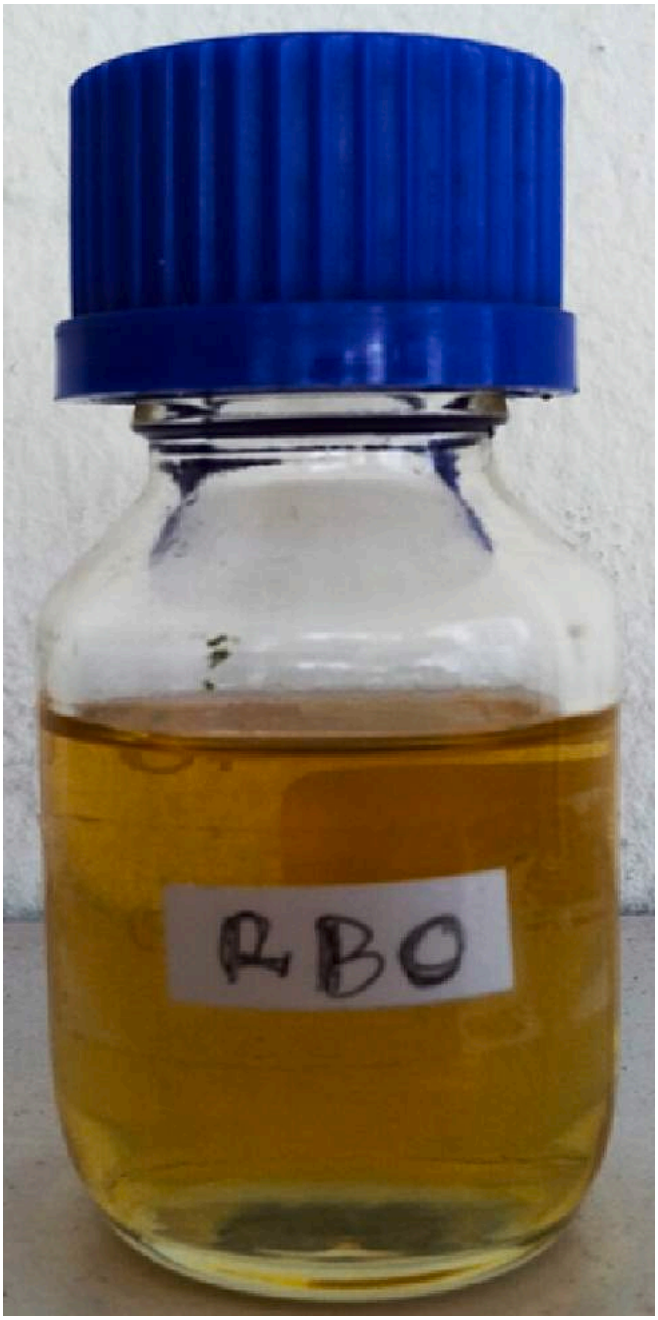

Fig. 2. Crude RBO.

Table 1
Properties of crude RBO.

Property	Unit	RBO
Kinematic viscosity at 40 °C	mm^2/s	40.97
Density at 15 °C	kg/m^3	922
Acid value	mg KOH/g	1.82
Higher heating value	MJ/kg	36.88

bran oil. Combining infrared and ultrasound will increase the process of mass transfer into the reactant molecules. Hence, the combination of these techniques is expected to further enhance the transesterification reaction rate. Three process variables, which are oil to methanol molar ratio, catalyst concentration and reaction time were considered in this optimization study. Initially, Box-Behnken experimental designs (BBD)

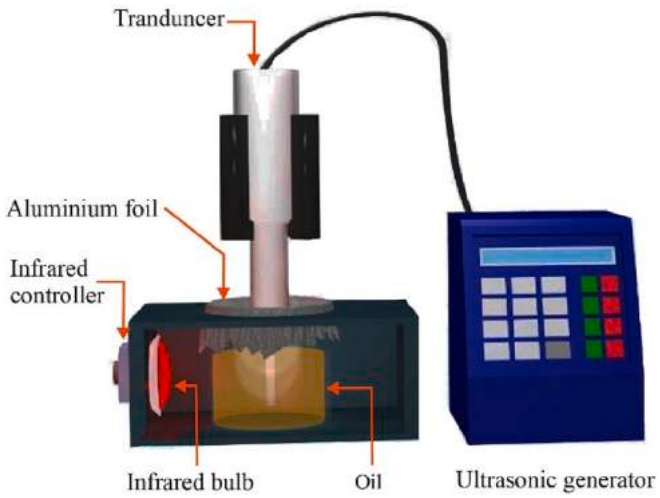

Fig. 3. Ultrasound and infrared radiation equipment system for biodiesel production.

was used in obtaining the experimental conditions. Data generated from BBD was subsequently supplied to the combination of ANN-GWO algorithm. In this study, GWO was utilized to optimize the weights of ANN. Subsequently, rice bran methyl ester (RBME) obtained via transesterification process was characterized accordingly using gas chromatographic with flame ionization detection (GC) and Fourier transform infrared spectrometry (FTIR). ASTM D6751 and EN 14214 standards were used to measure the properties of RBME. With the approach of combining ultrasonic and infrared, it is believed that there is a saving in energy, which allows future advancement in biodiesel production methods.

2. Materials and methods

2.1. Materials

Agricultural waste RBO was collected from Scienfield Sdn. Bhd. (Selangor, Malaysia). Methanol and potassium hydroxide (KOH) were supplied by Chemolab Supplies (Selangor, Malaysia). The chemicals were of analytical chemistry standard with 99% purity. The color of crude RBO is yellow bright (Fig. 2). Kinematic viscosity, acid value, higher heating value, and density of crude RBO are presented in Table 1.

2.2. Experimental Set-up

A 250 mL borosilicate glass beaker, aluminium foil, and thermometer were utilized in the biodiesel production reactor setup. Qsonica (Q500-20, 500 W, 20 kHz frequency) sonicator, equipped with a 1-inch probe was used to create the ultrasonic cavitation in the mixture. Amplitude and pulse of the sonicator were fixed at 35% and 6 s ON with 2 sec OFF, respectively. The system was fitted with 300 W infrared lamps (220 V) to produce infrared radiation. Infrared radiation is supplied with the intention to speed up the transesterification process. The set up box was covered with aluminium foil and connected to the ultrasound probe. The experimental setup of ultrasound combined with an infrared biodiesel synthesis schematic diagram is illustrated in Fig. 3.

2.3. Transesterification process

Quantity of methanol, KOH catalyst, and reaction time were selected for each run, which were planned using Box-Behnken design (BBD). RBO in the amount of 30 g was heated to 60 °C in the reactor using infrared radiation. After the oil had been heated to 60 °C, the ultrasound equipment was turned on, followed by slowing down the power of

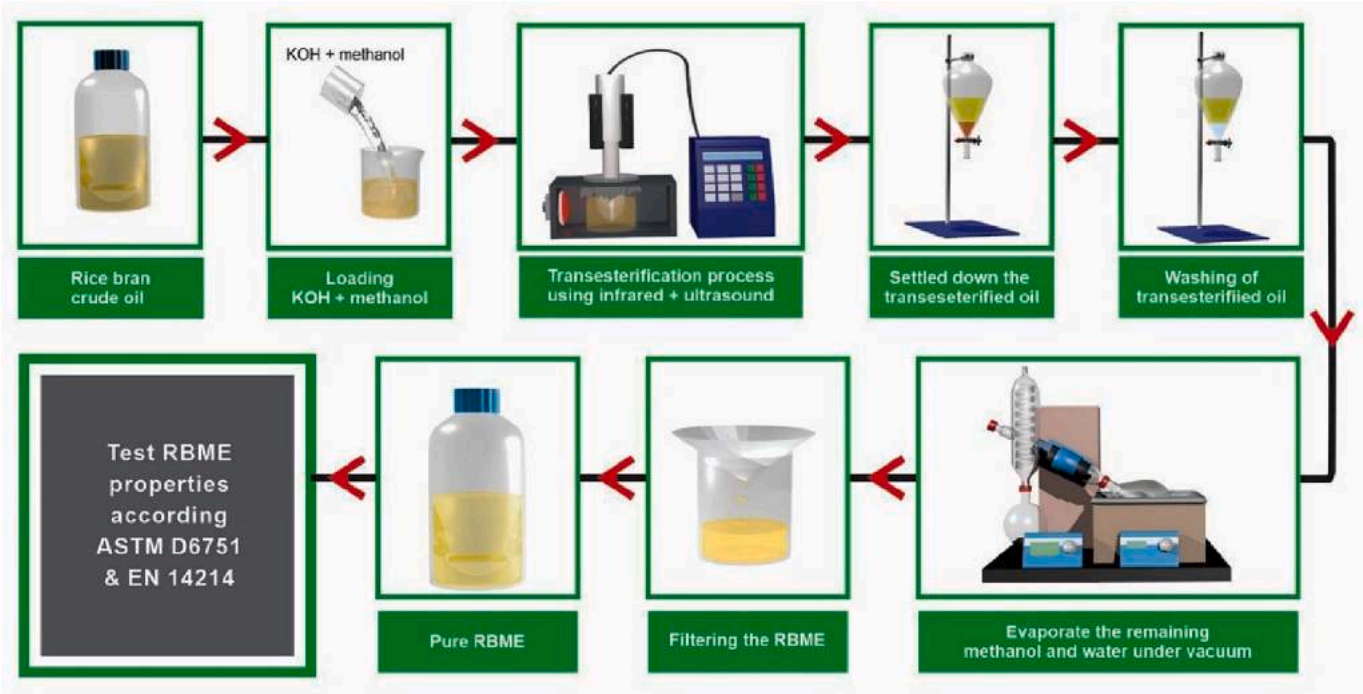

Fig. 4. Transesterification process using ultrasound combined with infrared radiation.

Table 2
Experimental conditions for methyl ester conversion using Box Behnken design.

Run	X_1:Time (min)	X_2:Methanol (%)	X_3: Catalyst (wt.%)
1	8	45	0.75
2	6	45	1.00
3	6	30	0.75
4	10	45	0.50
5	10	45	1.00
6	8	45	0.75
7	10	60	0.75
8	8	30	0.50
9	8	60	1.00
10	6	45	0.50
11	8	60	0.50
12	8	45	0.75
13	8	45	0.75
14	8	45	0.75
15	6	60	0.75
16	10	30	0.75
17	8	30	1.00

infrared bulb. The solution of methanol-catalyst at a certain quantity was then mixed in the reactor. The mixture was poured into a separating funnel upon completion of the transesterification reaction, and allowed to settle for six hours. The lower layer, which consists of catalyst and by-product were removed, and then deionized water at 40 °C was used to wash the end product to remove any impurities. Rotary evaporator equipped with a vacuum, set at 60 °C bath temperature was used to evaporate the moisture in the product. Subsequently, the final product was filtered using 541 Whatman filter paper. The processes of transesterification ais summarized in Fig. 4.

The yield (wt.%) was determined based on Eq. (2):

$$\text{Methyl ester yield (wt.\%)} = \frac{\text{Weight of methyl ester yield produced (g)} \times 100}{\text{Weight of crude oil used (g)}} \quad (2)$$

2.4. Box-behnken

The experiment was conducted using conditions suggested by the Box-Behnken designs (BBD) model, with reaction time, methanol to oil ratio, and catalyst concentration using ultrasound combined with infrared radiation to speed up the transesterification process, as shown in Table 2. The studied parameters were time of reaction (6, 8, 10 min), methanol to oil ratio (30, 45, 60 %) and catalyst concentration (0.5, 0.75, and 1 wt%). Data obtained from BBD were later supplied to the ANN-GWO model. Based on the study parameters and the various conditions, the number of trial with various condition is based on BBD as stated in Eq. (3).

$$N = 2k(k-1) + Nc \quad (3)$$

In Eq. (3), k and Nc are defined as the number of studied variables and number of central points, respectively [43]. MATLAB with neural networks and genetic algorithm toolboxes was used to formulate ANN and GWO modeling in optimizing the yield of RBME.

2.5. ANN modelling

MATLAB (Version 7.10, R2010a, MathWorks Inc., USA) was utilized to generate the ANN model. ANN modelling required 3 parts which are defined as input, hidden and output layer. Three neurons (one for each variables, namely methanol to oil ratio, catalyst concentration, and reaction time) were used for the input layer, but only one output neuron was used (RBME yield). The ANN model was fed with seventeen datasets from Table 2, each representing a unique combination of all the three variables considered in the study. 70%, 15%, and 15% from the data points were subsequently utilized for the purpose of training, validation, and testing, respectively. For training, Levenberg-Marquardt technique was used until the mean squared error (MSE) falls below a certain threshold. At the same time, the value of average correlation coefficient (R) was near to or exactly one.

2.6. Statistical evaluation of the developed models

As shown in Eqs. (4) and (5), other statistical metrics, such as

Table 3
Comparison of RBME yield between ultrasound, infrared irradiation and hybrid of ultrasound-infrared irradiation transesterification using the optimum process parameters.

Method	Experimental run	Time of reaction (min)	Methanol/oil ratio (%)	Catalyst (wt.%)	RBME (wt.%)		Standard error	Reference
					Predicted	Experimental		
Conventional[a]	1	60	6:1[b]	0.9	–	98.7	–	[48]
Ultrasound	1	48	6:1[b]	0.5	94.12	93.82	0.21	[31]
	2	48	6:1[b]	0.5	94.12	93.91		
	3	48	6:1[b]	0.5	94.12	94.22		
	Average				94.12	93.98		
Ultrasound + Infrared	1	7.76	60	1	98.16	97.79	0.21	This study
	2	7.76	60	1	98.16	97.93		
	3	7.76	60	1	98.16	97.51		
	Average				98.16	97.74		

[a] Reaction temperature was 60 °C.
[b] Methanol to oil molar ratio.

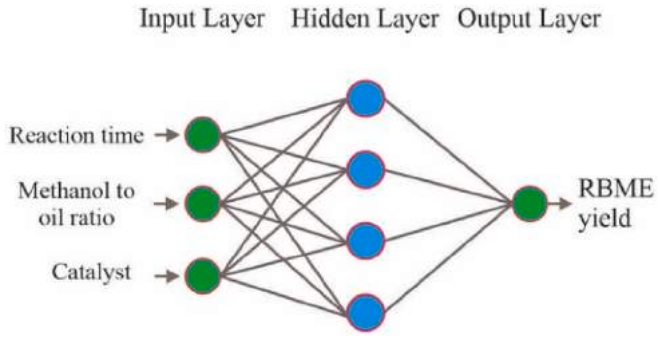

Fig. 5. Architecture of ANN model for RBME yield.

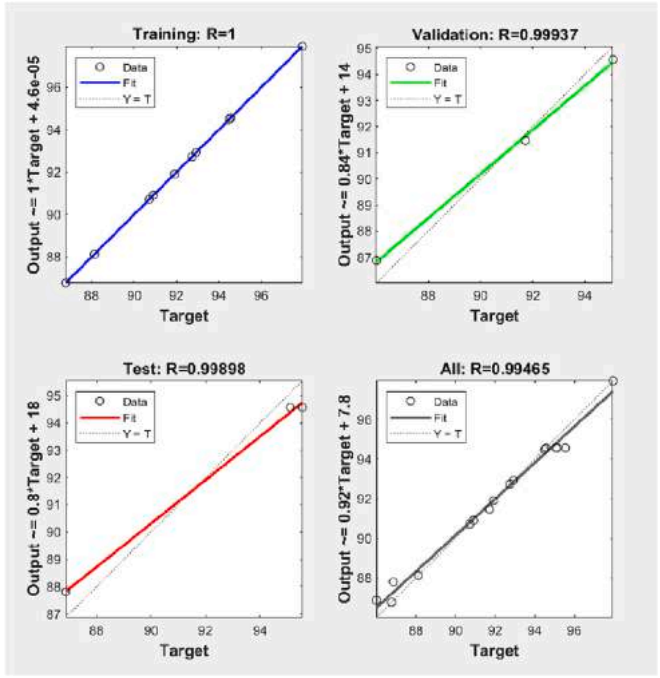

Fig. 6. The values for coefficient of correlation (R) obtained specifically for training, validation, testing and the overall datasets.

coefficient of determination (R^2) and root mean absolute error (RMSE) [44], were employed to test the proposed models.

$$R^2 = 1 - \frac{\sum_{i=1}^{n}(M_e - M_p)^2}{\sum_{i=1}^{n}(M_p - M_{avg})^2} \quad (4)$$

$$RMSE = \sqrt{\frac{1}{n}\sum_{i=1}^{n}(M_e - M_p)^2} \quad (5)$$

Here, n, M_p, M_e and M_{avg} are defined as number of points, predicted value, experimental value, and average experimental values, respectively.

2.7. Gwo

GWO was initially developed using the inspiration obtained from the behavior of a wolf pack when hunting for a prey. First level of the hierarchy consists of the alpha (α), while second, third, and lowest levels are referred to as beta (β), delta (δ), and omega (ω), respectively. The leader of the pack is referred as α, where the entire pack need to follow the decisions of the α. Some α has democratic behavior that follow the decision from other wolves in the pack. The lower rank wolf have to submit to the α. β will become α, after α gets old or passed away. β will also assists the α in decision-making and other activities. The wolves will submit to both α and β, but dominant than ω. Therefore, the lowest ranking wolves, ω, play the roles of a scapegoat [43].

Grey wolves hunting behaviour can be divided into three parts. They will hunt in a group by tracking and chasing the prey, then they will pursue, encircle and torture the prey until it no longer moves. Lastly, they will attack the prey. Hence, Eq. 6 is the developed functions based on the social hierarchy and behaviour of the grey wolf [38,45].

$X_i^d(t+1) = X_i^d(t) - A_i^d\left|C_i^d X_p^d(t) - X_i^d(t)\right|$ (6) Here, t, X_i, and X_p are defined as iterations, position vector of a grey wolf, and position vector of the prey, respectively. Moreover, $A_i^d = 2a.r_1 - a$, $C_i^d = 2.r_2, r_1 and r_2$ are random vectors in [0,1]. Here, the vector $\vec{a}$ is decreasing linearly from 2 to 0, which means a(t) = 2–2 t/*max_iter*, and *max_iter* is defined as the maximum iteration number. Eqs. (7)–(10) are used to update the position of ω, regardless the positions of α, β and δ

$$X_{i,\alpha}^d(t+1) = X_\alpha^d(t) - A_{i,1}^d\left|C_{i,1}^d X_\alpha^d(t) - X_i^d(t)\right| \quad (7)$$

$$X_{i,\beta}^d(t+1) = X_\beta^d(t) - A_{i,\beta}^d\left|C_{i,2}^d X_\beta^d(t) - X_i^d(t)\right| \quad (8)$$

$$X_{i,\delta}^d(t+1) = X_\delta^d(t) - A_{i,\delta}^d\left|C_{i,3}^d X_\delta^d(t) - X_i^d(t)\right| \quad (9)$$

$$X_i^d(t+1) = \frac{X_{i,\alpha}^d(t+1) + X_{i,\beta}^d(t+1) + X_{i,\delta}^d(t+1)}{3} \quad (10)$$

2.8. Optimization and validation

To acquire the best yield, ANN-GWO was utilized to predict the the optimum values of the three examined process parameters. Here, the values with the highest RBME yield for ANN were determined using

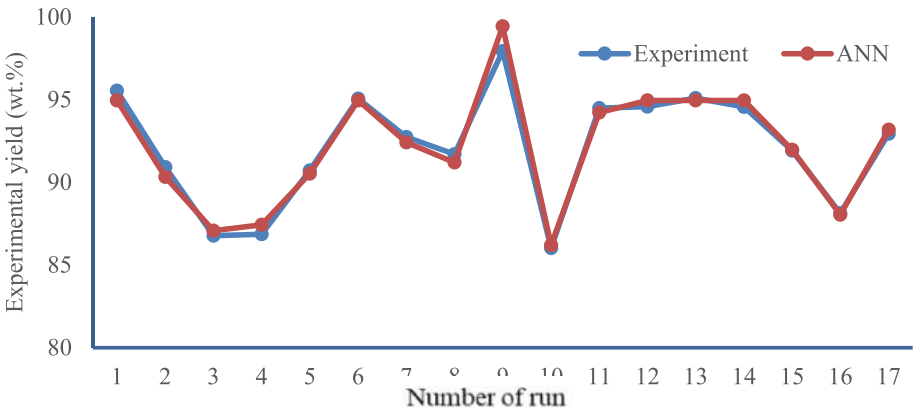

Fig. 7. Experimental vs prediction yield of RBME.

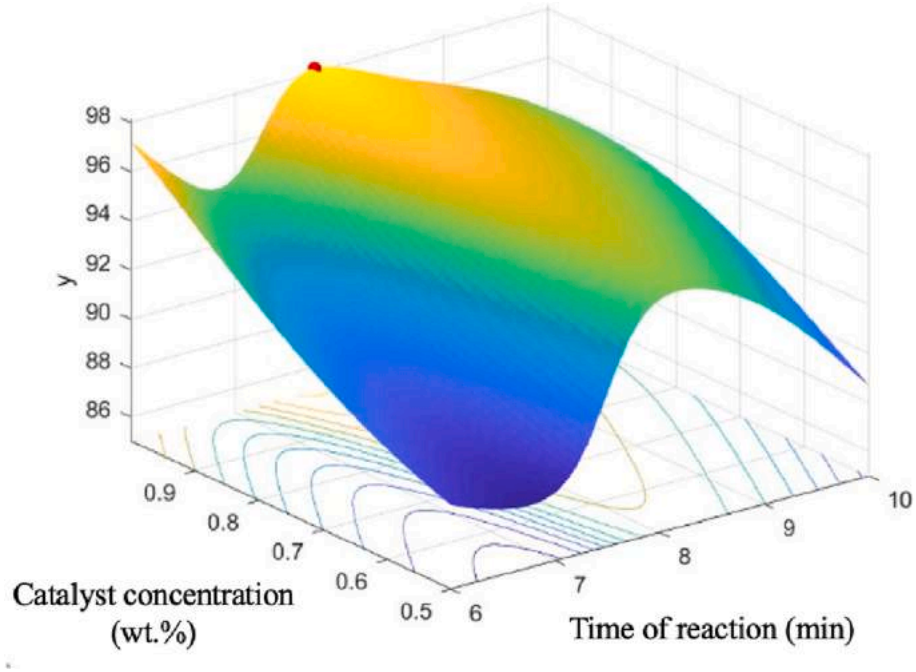

Fig. 8. Three-dimensional surface plots of reaction time and catalyst concentration.

GWO. The target values is determined by averaging the values by triple trials and compare it will the projected value.

2.9. Physicochemical properties of RBME

FTIR spectroscopy was applied to characterize the RBME. Subsequently, other properties of RBME were measured using ASTM D6751 and EN 14214 standards. Kinematic viscosity was measured using Anton Paar SVM3000 Stabinger Viscometer (Graz, Austria) at 40 °C while the density of RBME was measured using DM40 LiquiPhysics TM density meter (Mettler Toledo, Greifensee, Switzerland) at 15 °C. Calorific value was measured using Parr 6200 Isoperibol Calorimeter. Acid value was acquired by automation titration rondo 20 (Mettler Toledo, Switzerland).

3. Results and discussion

3.1. ANN modelling

A total of 17 experimental runs were carried out with three input variables: reaction time (6, 8 and 10 min), methanol to oil ratio (30, 45, and 60%), and catalyst concentration (0.5, 0.75, and 1.00 wt%), as well as one output variable: RBME. The result of output variable was shown in Fig. 7 and Table 3 tabulated the experimental design of this study where the data was acquired for training, validation and testing algorithm. Utilizing Levenberg–Marquardt algorithm model, 70%, 15% and 15% of the data was used for training, testing and validation, respectively. The three input neurons, four hidden neurons and one output neuron was used to train the algorithm as shown in Fig. 5. The optimal number of the hidden neurons was determined by a heuristic technique. The ANN prediction model with R for training, validation, test and all is 1, 0.999, 0.9989, and 0.9946, respectively, illustrated in Fig. 6. Furthermore, the lowest mean square error (MSE) of 0.251 was obtain this study. The prediction of ANN with BBD design on the output variable of RBME and the experimental shown in Fig. 7. The comparison revealed that the model suited the target values linearly and accurately. This suggests that the model was appropriate for accurately predicting the RBME output. The network projected values for the biodiesel transesterification process were found to be consistent with the actual experiment. This indicates the network's intrinsic sensitivity and

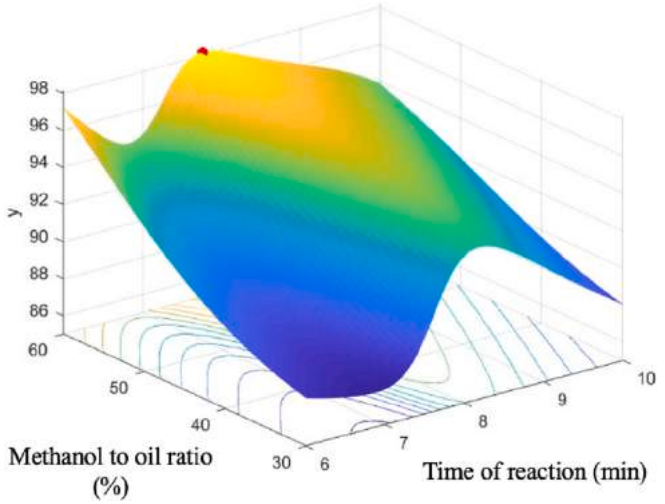

Fig. 9. Three-dimensional surface plots of reaction time and methanol to oil ratio.

precision in tracking the transesterification process simultaneously.

3.2. Interaction effects of reaction time and concentration of Catalyst.

Fig. 8 shows the interaction of reaction time and catalyst concentration in the transesterification of RBO. When the reaction time is prolonged from 6 to 7.76 min, it can be seen that the RBME yield increases up until a certain point. After the optimum point, it shows an significant decrease in the RBME yield. While, the catalyst concentration must be sufficient to facilitate the transesterification. Both parameter shows that they are both equally important to determining the optimum condition for the RBME yield. The time of reaction must be controlled in the specific range, because it was found that longer reaction time might actually reverse the transesterification process, leading to less methyl ester yield [46]. Consequently, the amount of glycerides in the target biodiesel will be higher than the biodiesel produced using optimal conditions.

3.3. Interaction effects between reaction time and methanol to oil ratio

Interation effects between reaction time and methanol to oil ratio is shown in Fig. 9. For this purpose, methanol to oil ratio was set between 30 and 60 % to study its effect on other studied parameters. It is found that the plot in Fig. 8 is very similar to Fig. 9. With the introduction of higher methanol to oil ratio, RBME yeild is observed to increase as well. Highest RBME yield can be obtained at the value of 60% for the methanol to oil ratio. One explanation for this is caused by the nature of miscibility between methanol and oil, where sufficient ratio must be made available in order to shorten the transesterification time, as miscibility will increase the contact between methenium and glycerides [18,47]. The time of reaction is found to be favourable at 7.76 min.

3.4. Interaction effects of methanol to oil ratio and catalyst concentration

Fig. 10 depicts the relationship between methanol to oil ratio and catalyst concentration. Here, methanol to oil ratio and catalyst loading were varied from 30 to 60%, and 0.5 to 1 wt%, respectively. It can be seen that low values of these two process parameters is not favorable as it will only produce approximately 90% of RBME yield. With increasing value of both parameters, it is observed that the RBME yield rises as well, eventually reaching 98.16%. Hence, from the surface plot, 1 wt% of catalyst concentration is considered as the most suitable option.

3.5. Optimization and validation of model

Effects of the three studied process variables are shown by the three dimensional surface plots. By observing the plots, optimum operating conditions for all the studied variables can be determined. In other words, with the help of ANN-GWO modelling and BBD experimental design, the optimum operating parameter for biodiesel conversion was obtained. The values of optimum operating parameters for RBME yield are as follows: methanol to oil ratio = 60%, catalyst concentration = 1

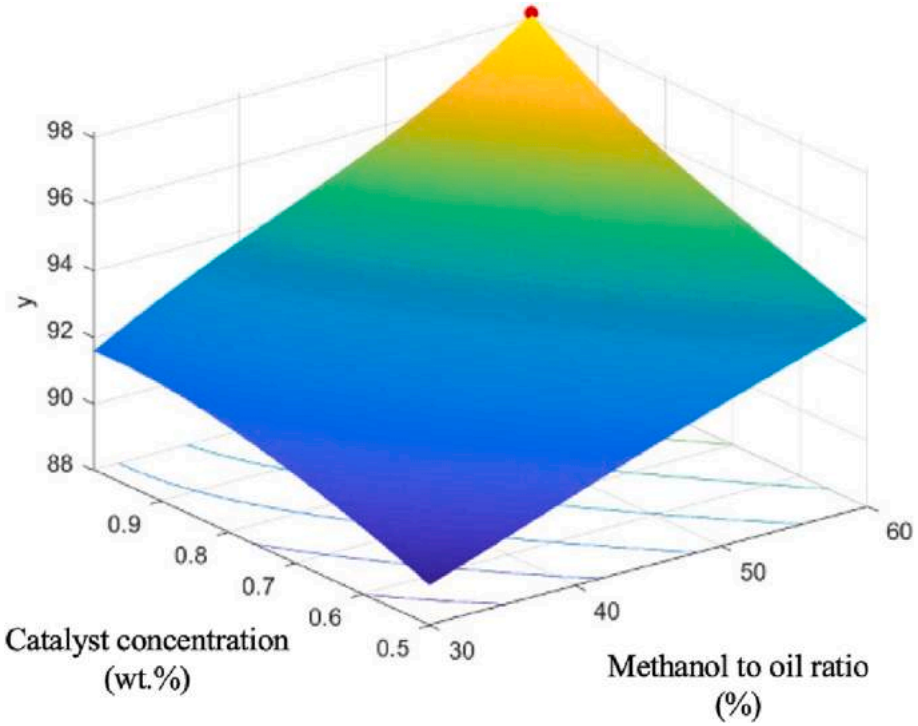

Fig. 10. Three-dimensional response surface plots of methanol to oil ratio and catalyst.

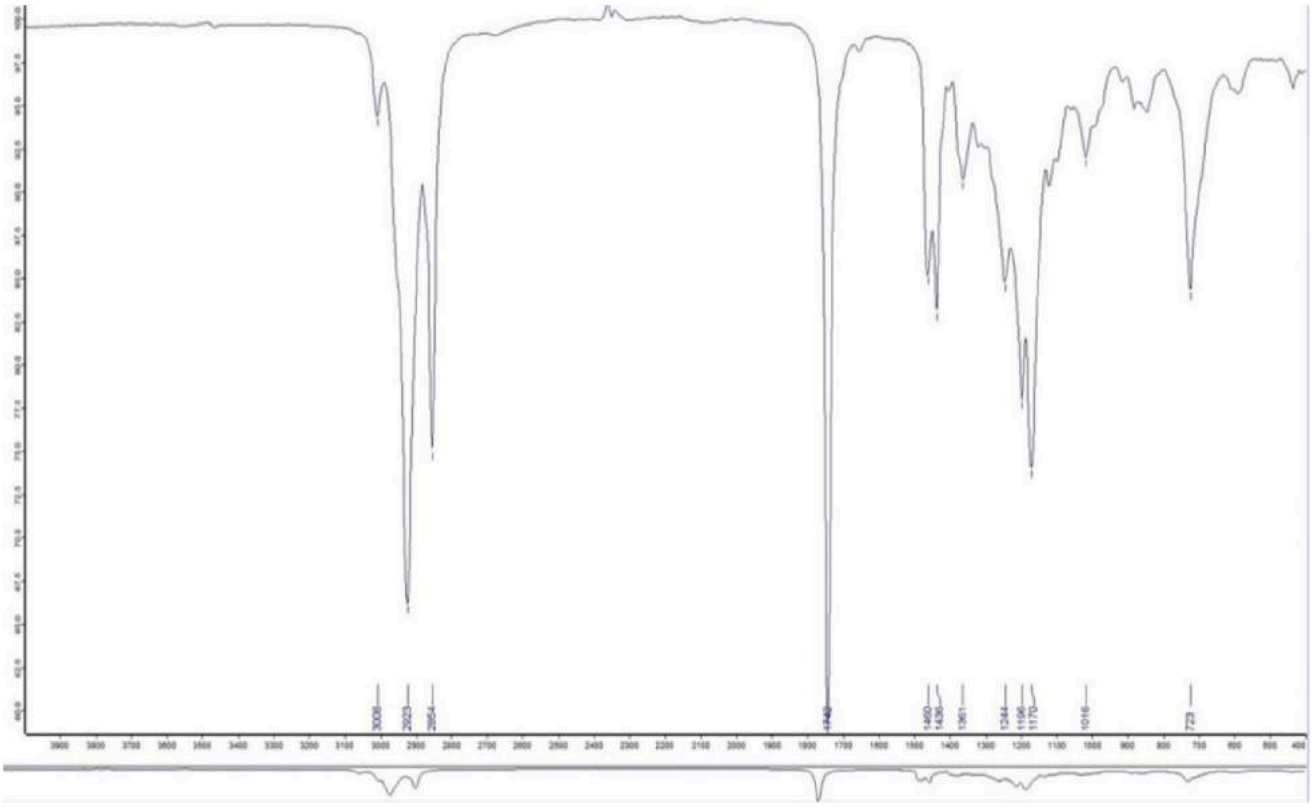

Fig. 11. FTIR spectra of RBME.

Table 4
FAME and linolenic methyl ester content of the RBME produced from Ultrasound and Infrared Radiation.

Name of FAME	Carbon amount	Area	Percentages
Methyl Octanoate	C8:0	202.813	3.72
Methyl Tetradecanoate	C14:0	20.334	0.37
Methyl Palmitate	C16:0	954.044	17.49
Methyl Octadecanoate	C18:0	101.850	1.87
Methyl cis − 9 - octadecenoate	C18:1	1981.401	36.32
Methyl Linoleate	C18:2 (CIS)	1701.202	31.18
Methyl Linolenate	C18:3	81.460	1.49
Methyl Arachidate	C20:0	50.325	0.92
Methyl Docosanoate	C22:0	16.762	0.31
Methyl Erucate	C22:1	46.858	0.86
Methyl Lignocerate	C24:0	25.919	0.48
FAME		95.00	
FAME- saturated		25.15	
FAME-unsaturated		69.85	

wt%, and reaction time = 7.76 min. Using the values, the maximum forecasted RBME yield is 98.16 wt%. Based on the above operating parametric conditions, the experiment was tri-replicated to validate the accuracy of the model and the average RBME yield obtained is 97.74 wt %. Based on the forecasted and experimental RBME yield, the difference was less than 0.41% with standard error of 0.21. This is a significant improvement to our previous study on ultrasound-assisted transesterification of rice bran oil, specifically for the optimum reaction time and methyl ester yield. Without the application of infrared in the previous study, the optimum reaction time was in the ultrasound-assisted reaction was found to be 48 min, with a yield of 94.12% [31]. Besides, using conventional heating to produce RBME required a longer optimum reaction time of 60 min and a catalyst of 0.9%. It found that the RBME yield for conventional is 98.7 wt% [48]. The detailed comparison of RBME yield using conventional, ultrasound, hybrid ultrasound and infrared irradiation is shown in Table 3. It can be observed that ultrasound irradiation only required a longer reaction time (~six times longer), and the yield obtained is slightly lower than the hybrid method by 3.76%. Then, it indicates that the hybrid method effectively facilitates transesterification because ultrasound promotes bubble implosion and infrared irradiation that provides instant heat. Finally, the hybrid method promotes the dispersion of oil molecules into smaller sizes and promotes better catalyst distribution, increasing accessibility to active sites that shorten the reaction time.

3.6. Ftir

FTIR can differentiate between crude oil and biodiesel and helps rapid analysis of liquid samples. Therefore, this research used ultrasound coupled with infrared for RBME production. The results were then studied by using FTIR and shown in Fig. 11. The functional group of

Table 5
Physical and chemical properties of RBME.

Property	Unit	Standard test method	ASTM D6751	En standards 14,214	Diesel	RBME	RBME [31]	RBME [48]
Kinematic viscosity at 40 °C	mm^2/s	D 445	1.9–6.0	3.5–5.0	2.86	4.88	4.8	4.12
Density at 15 °C	kg/m^3	D 1298	860–880	860–900	833	878	879.2	884
Acid value	mg KOH/g	D 664	Max. 0.5	Max 0.5	0.06	0.38	0.17	0.45
Higher heating value	MJ/kg	D 975	Min. 35	35	45.82	40.36	40.44	40

–COOH was shown by the three absorption bands which serve as a proof that the carboxylate is there. Intense absorption peak at 2923 cm^{-1} is attributed to the strongest carbonyl group's stretching (CH stretch), and absorption peak at 1742 cm^{-1} corresponds to the stretching of CO double bond [49]. Meanwhile, absoption peak at 1436 cm^{-1} is related to $–CH_3$ asymmetric stretch, while the peak at 1196 cm^{-1} corresponds to C-O-C asymmetric stretch [50]. Furthermore, the peak at 1,361 cm^{-1} in the FTIR spectrum is in line with $O-CH_3$ in glycerol that indicate the presence of the residual of the transesterification process. Absorption peaks with intensities between 1000 and 1800 cm^{-1} suggest a high FAME concentration in RBME.

3.7. FAME analysis

FAME analysis is one of the important methods to determine biodiesel's purity. Table 4 contains the FAME results obtained through gas. The results depends on the available fatty acid in the RBO, and it can be seen that methyl cis −9-octadecenoate (36.32%) and methyl linoleate (31.18%) are dominant FAME in RBME. The remaining methyl ester found were methyl palmitate (17.49%), methyl octanoate (3.72%), methyl octadecanoate (1.87%), methyl linolenate (1.49%), while others methyl ester compromised less than 1% of FAME content individually. The FAME's content has met the minimum requirement (>90%) stipulated in EN 14103: 2011. The RBME's saturated and unsaturated FAME contents were 25.15% and 69.85%, which compromised 95%. In comparison, the yield of the same feedstock was done by Mazaheri et al. is 92.38 wt% using a heterogeneous catalyst and heating mantle. Even though comparison can not be made under a similar process. Still, ultrasound coupled with infrared has shown better FAME production than the heating mantle. Saturated acids content promotes oxidation stability as the oxidation rate of saturated FAME is slower than that of unsaturated FAME [6,9].

3.8. RBME and RBO characterization

The properties of RBO and RBME fuel were evaluated and the results are tabulated in Table 5. The biodiesel produced from RBME in the range of all standards in EN 14214 and ASTM D6751 and was compared with RBME produced using ultrasound only [31] and conventional [48]. Therefore, RBME produced through ultrasound and infrared radiation-assisted shows better properties and it met the standard requirement stated by the ASTM D6751 and EN 14214. Consequently, this approach is viable for biodiesel production, as the RBME produced possesses the apropriate physicochemical qualities.

4. Conclusions

Biodiesel was produced from crude RBO using ultrasound combined with infrared radiation-assisted and assisted by ANN-GWO modelling. The optimization was performed based on three process parameters, namely methanol to oil ratio, catalyst concentration, and reaction time. The best parameters are obtained with reaction time of 7.76 min, methanol to oil ratio of 60%, and a 1 wt% catalyst concentration. The forecasted RBME based on the above conditions is 98.16, and the experimental result is 97.74 wt% with low standard error. From this study, it shows that ultrasound coupled with infrared radiation has improved the yield of biodiesel conversion. However, there is a particular limitation that must be taken into account, which was the capacity of the design equipment. Hence, we suggest to further investigate with a more powerful ultrasound, in meeting the capacity for industrial needs. Furthermore, this system is especially useful for transesterification using heterogeneous catalysts. Slow reaction rate involving heterogenous catalysts due to the existence of three-phase mixture (methanol-oil-catalyst) can be remedied with this combined system. Moreover, optimization using ANN-GWO modelling with BBD experimental design shows its value and accuracy in predicting the yield of RBME produced via the ultrasound coupled with infrared radiation system.

CRediT authorship contribution statement

A.H. Sebayang: Formal analysis, Validation. **Fitranto Kusumo:** Resources, Methodology. **Jassinnee Milano:** Conceptualization, Writing – review & editing. **A.H. Shamsuddin:** Funding acquisition, Supervision. **A.S. Silitonga:** Writing – original draft. **F. Ideris:** Investigation. **Joko Siswantoro:** Formal analysis, Validation. **Ibham Veza:** Investigation. **M. Mofijur:** Funding acquisition, Supervision. **Shir Reen Chia:** Conceptualization, Writing – review & editing.

Declaration of Competing Interest

The authors declare that they have no known competing financial interests or personal relationships that could have appeared to influence the work reported in this paper.

Data availability

The data that has been used is confidential.

Acknowledgments:

The authors wish to acknowledge financial support provided by AAIBE Chair of Renewable Energy, grant no: 202003 KETTHA and 201801 KETTHA. The authors wish to thank Centre of Green Technology, Faculty of Engineering and Information Technology, University of Technology Sydney and Centre of Renewable Energy, 2023 Strategy Research Support funding from the University of Technology Sydney, Sydney, Australia, and DIPA POLMED 2023 supported by Politeknik Negeri Medan, Medan, Indonesia.

Appendix A. Supplementary data

Supplementary data to this article can be found online at https://doi.org/10.1016/j.fuel.2023.128404.

References:

[1] Amin M, et al. Thermal properties of beeswax/graphene phase change material as energy storage for building applications. Appl Therm Eng 2017;112:273–80.
[2] Mehrali M, et al. Preparation and characterization of palmitic acid/graphene nanoplatelets composite with remarkable thermal conductivity as a novel shape-stabilized phase change material. Appl Therm Eng 2013;61(2):633–40.
[3] Pérez-Collazo C, Greaves D, Iglesias G. A review of combined wave and offshore wind energy. Renew Sustain Energy Rev 2015;42:141–53.
[4] Silitonga AS, et al. Intensification of Reutealis trisperma biodiesel production using infrared radiation: Simulation, optimisation and validation. Renew Energy 2019;133:520–7.
[5] Chia SR, et al. Sustainable approaches for algae utilisation in bioenergy production. Renew Energy 2018;129:838–52.
[6] Mazaheri H, et al. Rice bran oil based biodiesel production using calcium oxide catalyst derived from Chicoreus brunneus shell. Energy 2018;144:10–9.
[7] Mofijur M, et al. Comparative Evaluation of Edible and Non-edible Oil Methyl Ester Performance in a Vehicular Engine. Energy Procedia 2015;75:37–43.
[8] Mofijur M, et al. Prospects of biodiesel from Jatropha in Malaysia. Renew Sustain Energy Rev 2012;16(7):5007–20.
[9] Dharma S, et al. Optimization of biodiesel production process for mixed Jatropha curcas-Ceiba pentandra biodiesel using response surface methodology. Energ Conver Manage 2016;115:178–90.
[10] Silitonga AS, et al. A review on prospect of Jatropha curcas for biodiesel in Indonesia. Renew Sustain Energy Rev 2011;15(8):3733–56.
[11] Silitonga AS, et al. Evaluation of the engine performance and exhaust emissions of biodiesel-bioethanol-diesel blends using kernel-based extreme learning machine. Energy 2018;159:1075–87.
[12] Mofijur M, et al. Evaluation of biodiesel blending, engine performance and emissions characteristics of Jatropha curcas methyl ester: Malaysian perspective. Energy 2013;55:879–87.
[13] Azeem MW, et al. Production of biodiesel from low priced, renewable and abundant date seed oil. Renew Energy 2016;86:124–32.
[14] Uddin MN, et al. An Overview of Recent Developments in Biomass Pyrolysis Technologies. Energies 2018;11(11).

[15] Ong HC, et al. Optimization of biodiesel production and engine performance from high free fatty acid Calophyllum inophyllum oil in CI diesel engine. Energ Conver Manage 2014;81:30–40.
[16] Ong HC, et al. Physicochemical properties of biodiesel synthesised from grape seed, Philippine tung, kesambi, and palm oils. Energies 2020;16(3).
[17] Chakraborty R, Sahu H. Intensification of biodiesel production from waste goat tallow using infrared radiation: Process evaluation through response surface methodology and artificial neural network. Appl Energy 2014;114:827–36.
[18] Milano J, et al. Optimization of biodiesel production by microwave irradiation-assisted transesterification for waste cooking oil-Calophyllum inophyllum oil via response surface methodology. Energ Conver Manage 2018;158:400–15.
[19] Martinez-Guerra E, Gude VG. Transesterification of used vegetable oil catalyzed by barium oxide under simultaneous microwave and ultrasound irradiations. Energ Conver Manage 2014;88:633–40.
[20] Koutsouki AA, et al. In situ and conventional transesterification of rapeseeds for biodiesel production: The effect of direct sonication. Ind Crop Prod 2016;84:399–407.
[21] Chipurici P, et al. Ultrasonic, hydrodynamic and microwave biodiesel synthesis – A comparative study for continuous process. Ultrason Sonochem 2019;57:38–47.
[22] Ideris F, et al. Optimization of ultrasound-assisted oil extraction from Canarium odontophyllum kernel as a novel biodiesel feedstock. J Clean Prod 2021;288.
[23] Tan SX, et al. State of the art review on development of ultrasound-assisted catalytic transesterification process for biodiesel production. Fuel 2019;235:886–907.
[24] R, C., *Indian Patent Application*. 2012: India.
[25] Pradhan P, Chakraborty S, Chakraborty R. Optimization of infrared radiated fast and energy-efficient biodiesel production from waste mustard oil catalyzed by Amberlyst 15: Engine performance and emission quality assessments. Fuel 2016;173:60–8.
[26] Hanif M, et al. Energ y saving potential using elite jatropha curcas hybrid for biodiesel production i n Malaysia. Int J Recent Technol Eng 2019;8:6281–7.
[27] Tan SX, et al. Process intensification of biodiesel synthesis via ultrasound-assisted in situ esterification of Jatropha oil seeds. J Chem Technol Biotechnol 2019;94(5):1362–73.
[28] Godwin John J, et al. Waste cooking oil biodiesel with FeO nanoparticle – A viable alternative fuel source. Mater Today: Proc 2023;72:1991–5.
[29] Aryasomayajula Venkata Satya Lakshmi SB, et al. Biodiesel production from rubber seed oil using calcined eggshells impregnated with Al2O3 as heterogeneous catalyst: A comparative study of RSM and ANN optimization. Braz J Chem Eng 2020;37(2):351–68.
[30] Goh BHH, et al. Ultrasonic assisted oil extraction and biodiesel synthesis of Spent Coffee Ground. Fuel 2020;261:116121.
[31] Ibrahim H, et al. An ultrasound assisted transesterification to optimize biodiesel production from rice bran oil. Mech Eng 2020;11(2):225–34.
[32] Zaidel, D.N.A., et al., *18 - Production of biodiesel from rice bran oil*, in *Biomass, Biopolymer-Based Materials, and Bioenergy*, D. Verma, et al., Editors. 2019, Woodhead Publishing. p. 409-447.
[33] Xu, X. and L. Cheong, *Preface*, in *Rice Bran and Rice Bran Oil*, L.-Z. Cheong and X. Xu, Editors. 2019, AOCS Press. p. xi-xiii.
[34] Hoang AT, et al. Rice bran oil-based biodiesel as a promising renewable fuel alternative to petrodiesel: A review. Renew Sustain Energy Rev 2021;135:110204.
[35] Lourenço VA, et al. Investigation of ethyl biodiesel via transesterification of rice bran oil: bioenergy from residual biomass in Pelotas, Rio Grande do Sul - Brazil. Renew Sustain Energy Rev 2021;144:111016.
[36] Kusumo F, et al. A comparative study of ultrasound and infrared transesterification of Sterculia foetida oil for biodiesel production. Energy Sources Part A 2017;39(13):1339–46.
[37] Liyanaarachchi VC, et al. Development of an artificial neural network model to simulate the growth of microalga Chlorella vulgaris incorporating the effect of micronutrients. J Biotechnol 2020;312:44–55.
[38] Ong MY, et al. Modeling and optimization of microwave-based bio-jet fuel from coconut oil: Investigation of response surface methodology (rsm) and artificial neural network methodology (ann). Energies 2021;14(2).
[39] Faizollahzadeh Ardabili S, et al. Computational intelligence approach for modeling hydrogen production: a review. Eng Appl Comput Fluid Mechanics 2018;12(1):438–58.
[40] Kolakoti A, Satish G. Biodiesel production from low-grade oil using heterogeneous catalyst: an optimisation and ANN modelling. Aust J Mech Eng 2020:1–13.
[41] Onukwuli O, et al. Comparative analysis of the application of artificial neural network-genetic algorithm and response surface methods-desirability function for predicting the optimal conditions for biodiesel synthesis from chrysophyllum albidum seed oil. J Taiwan Inst Chem Eng 2021;125.
[42] Nasrudin MF, et al. Sardine feast metaheuristic optimization: An algorithm based on sardine feeding frenzy. J Theor Appl Inf Technol 2021;99(17):4349–57.
[43] Mirjalili S, Mirjalili SM, Lewis A. Grey Wolf Optimizer. Adv Eng Softw 2014;69:46–61.
[44] Panda, M. and B. Das. *Grey Wolf Optimizer and Its Applications: A Survey*. in *Proceedings of the Third International Conference on Microelectronics, Computing and Communication Systems*. 2019. Singapore: Springer Singapore.
[45] Kundu P, et al. Formulation development, modeling and optimization of emulsification process using evolving RSM coupled hybrid ANN-GA framework. Chem Eng Res Des 2015;104:773–90.
[46] Sukpancharoen S, et al. Unlocking the Potential of Transesterification Catalysts in Biodiesel Production through Machine Learning Approach. Bioresour Technol 2023:128961.
[47] Musa IA. The effects of alcohol to oil molar ratios and the type of alcohol on biodiesel production using transesterification process. Egypt J Pet 2016;25(1):21–31.
[48] Lin L, et al. Biodiesel production from crude rice bran oil and properties as fuel. Appl Energy 2009;86(5):681–8.
[49] Peña AG, et al. Fourier transform infrared-attenuated total reflectance (FTIR-ATR) spectroscopy and chemometric techniques for the determination of adulteration in petrodiesel/biodiesel blends. Quim Nova 2014;37:392–7.
[50] Zamba ZZ, Reshad AS. Synthesis of fatty acid methyl ester from Croton macrostachyus (bisana) kernel oil: parameter optimization, engine performance, and emission characteristics for Croton macrostachyus kernel oil fatty acid methyl ester blend with mineral diesel fuel. ACS Omega 2022;7(24):20619–33.